Dietary fibers with different viscosity regulate lipid metabolism via ampk pathway: roles of gut microbiota and short-chain fatty acid

Yu Li,*,†,1 Daiyang Xia,*,1 Jianying Chen,* Xiufen Zhang,* Heng Wang,* Liang Huang,* Jiajia Shen,*
Shunxiang Wang,§ Yan Feng,§ Danyan He,§ Jiaqing Wang,‡ Hui Ye,* Yongwen Zhu,* Lin Yang,* and
Wence Wang*,2

*Guangdong Provincial Key Laboratory of Animal Nutrition and Regulation, College of Animal Science, South China Agricultural University, Guangzhou 510642, China; †Department of Animal Science, Guangdong Maoming Agriculture & Forestry Technical College, Maoming 525000, China; ‡Guangdong Haida Group Co. Ltd., Guangzhou 510535, China; and §Gold Coin Feedmill (Dong Guan) Co. Ltd, Dongguan 52300, China

ABSTRACT Dietary fiber (**DF**) improves gastrointestinal health and has important associations with the alleviation of intestinal diseases and metabolic syndrome. However, due to DFs complex characteristics, such as solubility, viscosity, and fermentability, the mechanism in these was not consistent. As an herbivore, the goose has a prominent digestive ability to DF. Therefore, we choose low, medium, and high viscosity DFs (respectively resistant starch-3 [|**RS**], inulin [**INU**], and β−glucan [**GLU**]) as Magang goose diet treatment for 4 wk, to investigate the effect and potential mechanism of different viscosities DFs on the growth and development process of goose.

In summary, three degrees of viscous DFs could decrease the mechanismic lipid level of geese by promoting acid-producing bacteria and short-chain fatty acid (**SCFA**) production, therefore, activating AMPK pathway-related genes through the gut-liver axis. High viscous DF has a greater lipid-lowering effect on geese, while medium viscous DF has preferable intestinal mucosal protection.

Key words: dietary fiber, gut microbiota, SCFAs, lipid metabolism, AMPK

INTRODUCTION

DF is defined as a large group of polysaccharide components that play an important role in gastrointestinal health, nutrient mechanism, and various diseases in the host. DFs have complex physicochemical characteristics and functions due to their widespread sources and structures (Honda et al., 2011). The polymer subunits, linkages, structures, and side chains determine DFs solubility, viscosity, and fermentability. Observational studies revealed that DF viscosity has close associations with SCFA production, and therefore modulate the luminal pH and control intestinal pathogens growth. Consumption of viscous DF also alters transit time in the upper gut, including decreasing gastric emptying rate and modulating small intestinal transit (Müller et al., 2018).

Long term high-fat diet is one of the important factors of lipid metabolism disorder, which will result in abnormalities in the quality and quantity of lipids and their metabolites. Dysregulation of lipid metabolism has been verified as the main cause of many diseases, including obesity, non-alcoholic fatty liver disease (**NAFLD**), cardiovascular diseases, insulin resistance, hypertension, and atherosclerosis (Delitala et al., 2017; Engeli et al., 2018). Increasing evidence has shown that intestinal microbiota composition and the ratio of SCFA play important roles in the progress of obesity and metabolic syndromes (Paturi et al., 2010; Bäckhed and Sonnenburg, 2016; Wang et al., 2016). SCFA, especially butyric acid, could improve insulin resistance in mice fed a high-fat diet, and its possible mechanism is to maintain mitochondrial activity and energy consumption which needs further investigation (Gao et al., 2009). Human and animal studies proved that varieties and contents of SCFA were precisely modulated by discrete DF structures in diets. Even though both soluble and insoluble DFs showed certain extent cholesterol-adsorption capacities and prebiotic effects, viscosity is more apparent than the quantity of DF related with lipid-lowering effects among individuals (Wu et al., 2020). But the function of DF viscosity in the small intestine is less well investigated.

Unlike with some mammals and other poultry, the goose has its characteristics of digesting a high-fiber diet, with prominent hydrolysis ability in cecum for plant-based chemical bonds of DF (Zhou et al., 2018). Few studies have been investigated the effects of DFs with different viscosities on the prevention of lipid accumulation and its mechanism in poultry. With high fermentability, inulin, β-glucan, and resistant starch widely existed in natural DFs, which have different viscosities. Most studies investigated the impact of DFs in the form of natural resources, such as cereal, forage, or crops. Effects of DFs were various due to the complex characteristics and components of natural plants. Therefore, we used purified compounds of DFs in our experiment. We hypothesized that different viscoelastic DFs may have different effects on SCFA production and the bacterial community of geese, therefore impact the fatty acid synthesis and cholesterol level in geese. This study may explore the potential mechanism and the pathway of DFs regulation in liver lipid metabolism involved intestinal microorganisms and SCFA.

MATERIALS AND METHODS

Animal, Diets, and Experimental Design

All practices and procedures for this experiment were reviewed and approved by the Animal Care and Use Committee of South China Agricultural University (SCAU-10564). Bentonite, resistant starch-3 (CAS No.: 13718-26-8, purity >99%), inulin (CAS No.: 9005-80-5, purity >90%), and $\beta-$glucan (CAS No.: 9041-22-9, purity >80%) used in the experiment were purchased from Shanghai Yuanye Biotechnology Co., Ltd. Magang geese in this experiment were purchased from Guangdong Haida Group Co., Ltd. A total of 576 fourteen-day-old Magang geese (male and female half) were randomly divided into 4 treatments, and each treatment contained 8 replicated with 18 geese in each replicate. Control (**CON**) group was fed with basal diet, 3 treatment groups contained different fiber ingredients, including 4% low-viscosity RS, 4% medium-viscosity INU, and 4 % high-viscosity GLU, respectively. All geese were kept in stainless steel cages (18 geese/cage), free drinking water and feed during the period, and kept under controlled room (temperature, maintained at $33 \pm 1°C$ for the first 3 d and then reduced by $2.5 \pm 0.5°C$ per week to a final temperature of 26°C; relative humidity, 45 to 60%; lighting, 24 h lighting with 10 Lux). The experimental period lasted for 4 wk. At 42 d of age, the birds were weighed, and the feed consumption and mortality were recorded for each replicate pen. The average daily gain (**ADG**), average daily feed intake (**ADFI**), and the ratio of feed to gain (**F/G**) were calculated. The composition and nutritional levels of the diets are shown in TableS1.

Sample Collection

We selected the geese with the nearest average body weight from each pen for sampling. Blood samples of approximately 10 mL, were collected at 42 d of age from 6 geese in each treatment group. Plasma was prepared by centrifuging the blood at 3,000 r/min for 10 mins and then stored at $-20°C$. The middle part of liver samples was collected after the phosphate-buffered saline (**PBS)** washing. Tissue samples of geese were collected for further analysis. The cecum digesta were collected and stored at $-80°C$ for further analyses. The cecum digesta sample was used for DNA extraction and subsequent microbial quantification.

Analysis of Biochemical Marker

Plasma contents of triglyceride (**TG**), total cholesterol (**TC**), high-density lipoprotein (**HDL**), and low-density lipoprotein (**LDL**) were detected by a fully automatic biochemical analyzer (AU480; Beckman Coulter, Inc., Brea, CA). Other liver biochemical indexes were measured using enzymatic kits from Nanjing Jiancheng Bioengineering Institute (Nanjing, China).

Analysis of Intestinal Mucosa Morphology

The duodenal, jejunal, and ileal samples were douched with physiologic saline and stored in 4% paraformaldehyde solution. The preserved segments were prepared after staining with hematoxylin and eosin (**HE**) solution using standard paraffin embedding procedures. Ten intact, well-oriented crypt-villus units were selected in triplicate as sources of each goose intestine cross-section. Morphometric variables, including villus height and crypt depth, were measured with an image processing and analysis system (Image Pro Plus, Media Cybernetics, Bethesda, MD).

Analysis of SCFA Concentrations

The contents of SCFA (total SCFA, acetic acid, propionic acid, butyric acid, isobutyric acid, valeric acid, and isovaleric acid) in cecal chyme were determined by gas chromatography. The instruments used in the determination process were gas chromatograph (model GC-6800, Beijing Beifen Tianpu Instrument Technology Co., Ltd.), Φ 6 mm $\times$ 2 m quartz glass packed column (stationary phase 15% FFAP, support 80-100 mesh Chromosorb), N-2000 chromatographic workstation, 10Ml tip microinjector (Shanghai Anting instrument factory). The chromatographic standards were as follows: acetic acid (Sigma A6283), propionic acid (Sigma P1386), butyric acid (Adlrich B103500), isobutyric acid (Adlrich 129542), isovaleric acid (Sigma I1754), valeric acid (Sigma V9769), and 2-ethylbutyric acid (Aldrich 10995-9). Metaphosphoric acid was the commercial analytical pure product.

Sample processing steps:1) Clarify the fermentation broth sample and centrifuge to remove particles and impurities (5,400 rpm × 10 min); 2) Add 1 mL of centrifugation supernatant and 0.2 mL of 25% metaphosphoric acid solution containing internal standard 2 EB

into 1.5 mL centrifuge tube, mix well, and freeze overnight at $-20°C$; 3) Centrifugation again (10,000 rpm $\times$ 10 min). The protein precipitate in the sample was removed and the supernatant was taken for use; 4) The chromatographic conditions of gas chromatograph are as follows: Φ 6 mm $\times$ 2 m quartz glass packed column (stationary phase 15% FFAP, support 80-100 mesh Chromosorb), column temperature 150°C, inlet temperature 220°C; Injection volume 1 μL, The temperature of FID detector is 280°C; the carrier gas is high purity N_2, the flow rate is 30 mL/min, and the pressure is 200 kPa; the gas is H_2 with a flow rate of 30 mL/min; the auxiliary gas is air with a flow rate of 300 mL/min.

Transcriptional Analysis

Total RNA was extracted from the frozen tissues using Magen HiPure Universal RNA Mini Kit (Magen, Guangzhou, China). The synthesis of the first strand (cDNA) was performed using oligo (dT) 20 and Superscript II reverse transcriptase (Takara, Japan). The sequence of primers used in real-time PCR assays is shown in Table S2. Real-time PCR was performed in an ABI 7500 (Applied Bio-systems, Foster City, CA) using SYBR Green Quantitative PCR kit (TaKaRa). The thermal cycling conditions consisted of one cycle at 95°C for 30 s followed by 40 cycles at 95°C for 5 s and 60°C for 34 s. The mRNA expression of each gene was calculated by the $2^{-\Delta\Delta Ct}$ method. β-actin was used as an internal control to normalize target gene transcriptional levels.

Microbial Diversity Analysis

DNA Extraction and PCR Amplification Microbial DNA was extracted from cecal digestion samples using the E.Z.N.A soil DNA Kit (Omega Bio-Tek, Norcross, GA) according to manufacturer protocols. The final DNA concentration and purification were determined by NanoDrop 2000 UV-vis spectrophotometer (Thermo Scientific, Wilmington, NC), and DNA quality was checked by 1% agarose gel electrophoresis. The V3-V4 hypervariable regions of the bacteria 16S rRNA gene were amplified with primers 338F (5'- ACTCCTACGG-GAG-GCAGCAG-3') and 806R (5'-GGAC-TACHVGGGT-WTCTAA T-3') by thermocycler PCR system (GeneAmp 9700, ABI). The PCR reactions were conducted using the following program: 3 mins of denaturation at 95°C, 27 cycles of 30 s at 95°C, 30 s for annealing at 55°C, and 45 s for elongation at 72°C, and a final extension at 72°C for 10 mins. PCR reactions were performed in triplicate 20 μL mixture containing 4 μL of 5 $\times$ FastPfu Buffer, 2 μL of 2.5 mM dNTPs, 0.8 μL of each primer (5 μM), 0.4 μL of FastPfu Polymerase and 10 ng of template DNA. The resulted PCR products were extracted from a 2% agarose gel and further purified using the AxyPrep DNA Gel Extraction Kit (Axygen Biosciences, Union City, CA) and quantified using QuantiFluor-ST (Promega) according to the manufacturer's protocol.

Illumina MiSeq Sequencing

Purified amplicons were pooled in equimolar and paired-end sequenced (2 $\times$ 300) on an Illumina MiSeq platform (Illumina, San Diego, CA) according to the standard protocols by Majorbio Bio-Pharm Technology Co. Ltd. (Shanghai, China).

Processing of Sequencing Data Raw fastq files were demultiplexed, quality-filtered by Trimmomatic, and merged by FLASH with the following criteria: 1) The reads were truncated at any site receiving an average quality score <20 over a 50 bp sliding window. 2) Primers were exactly matched allowing 2 nucleotide mismatching, and reads containing ambiguous bases were removed. 3) Sequences whose overlap longer than 10 bp were merged according to their overlap sequence. Operational taxonomic units (**OTUs**) were clustered with 97% similarity cutoff using UPARSE (version 7.1 http://drive5.com/uparse/) and chimeric sequences were identified and removed using UCHIME. The taxonomy of each 16S rRNA gene sequence was analyzed by RDP Classifier algorithm (http://rdp.cme.msu.edu/) against the Silva (SSU123) 16S rRNA database using confidence threshold of 70%.

Statistical Analysis

The data are expressed as mean $\pm$ SEM and analyzed using SAS 9.2 (SAS Inst. Inc., Cary, NC). Significant differences between the two groups were evaluated by two-tailed unpaired Student's t test or Mann-Whitney U test for samples that were not normally distributed. Significant differences among 3 or more groups were evaluated by one-way ANOVA with Bonferroni's multiple comparisons test. The level of significance was set at $P < 0.05$; *, $P < 0.05$; **, $P < 0.01$; ***, $P < 0.001$.

RESULTS

Influences of DFs on Growth Performance and Gastrointestinal Development

The growth performance of 15 to 42-day old Magang geese with different DF diets was shown in Figures 1A $-$1D. Compared with the CON group, the average final weight, ADFI, and ADG in the GLU group were extremely decreased ($P < 0.01$), while the F/G of the GLU group was significantly higher than that of the CON group. There was no significant difference in growth performance among the CON and other groups. The relative lengths of the duodenum, jejunum, and ileum in the GLU group were significantly higher than those in the CON group ($P < 0.01$), while the relative length of the cecum in the INU group was slightly higher than that in the CON group ($P = 0.072$). The relative weights of jejunum and ileum in the GLU group were significantly higher than those in the CON group ($P < 0.01$).
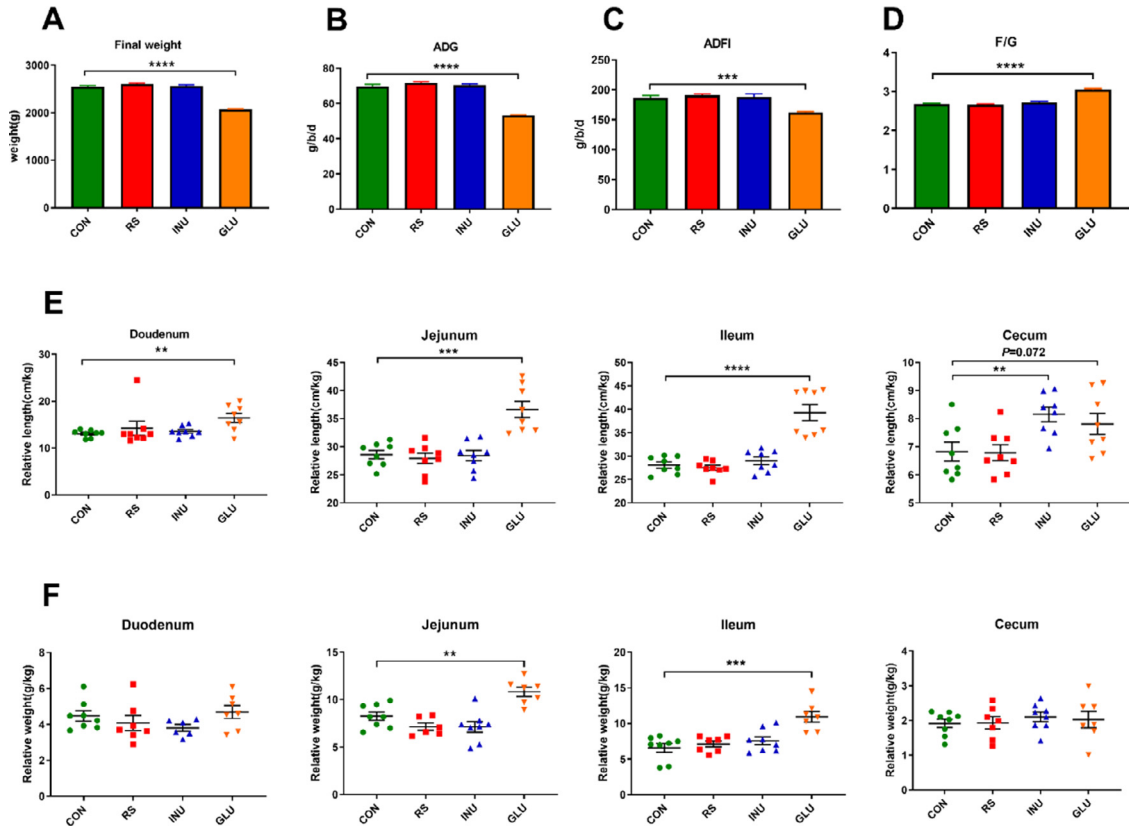
Figure 1. Effect of different DF on (A) Final weigh (B) ADG, (C) ADFI, (D) F/G of 15 to 42-day-old Magang geese. (E) Effect of different DF on the relative length of intestine on d 28 Magang geese (n = 8, mean with SEM). (F) Effect of different DF on the relative weight of intestine in 15 to 42-day-old Magang geese (n = 8, mean with SEM). Data were analyzed with unpaired t test, $*P < 0.05$, $**P < 0.01$, $*** P < 0.001$. Abbreviations: ADFI, average daily feed intake; DF, dietary fiber; ADG, average daily gain; F/G, feed/gain ratio.

Different DFs Modulated Lipid Homeostasis

Effects of different DFs on serum lipid metabolism-related biochemical indexes of 15 to 42-day-old Magang geese are shown in Figure 2A. Compared with the CON group, serum HDL-C levels in INU, GLU, and RS groups were significantly decreased ($P < 0.05$ or $P < 0.01$), serum malondialdehyde (**MDA**) levels in DF groups were significantly decreased ($P < 0.05$ or $P < 0.01$), while serum TC, TG, and LDL-C level in each group had no significant differences. Effects of different DFs on liver lipid metabolism-related biochemical indexes of Magang geese aged 15 to 42 d are shown in Figure 2B. Levels of TC and TG in the liver of the INU group were significantly lower than those in the CON group ($P < 0.05$). GLU had lower TC ($P < 0.01$) and TG ($P < 0.05$) levels in the liver, compared to the CON group. Compared with the CON group, the liver MDA level were significantly decreased in INU ($P < 0.01$), GLU ($P = 0.067$), and RS groups ($P < 0.05$). There were no significant differences in liver HDL-C and LDL-C levels among all groups.

Effects of different DFs on the mRNA expression related to liver lipid metabolism in Magang geese aged 15 to 42 d are shown in Figure 2C. Relative to CON group, liver *AMPKα, PPARα,* and carnitine palmitoyl-transferase-1 (***CPT*-1**) mRNA expression were significantly increased in INU, GLU, and RS groups ($P <$ 0.05); *SREBP1-c* and *ChREBP* expressions were significantly decreased in INU, GLU, and RS groups ($P < 0.05$ or $P < 0.01$); *ACC* expression was significantly decreased in the INU and GLU groups ($P < 0.01$); *FAS* has the decreased tendency in the INU ($P = 0.053$) and GLU groups ($P = 0.056$). However, there was no significant difference in *ACOX* and *CYP7A1* expressions among all groups.

DFs Significantly Improves the Intestinal Morphology and Protects the Intestinal Mucosa

The intestinal morphology of 15 to 42-day-old Magang geese fed with different types of DFs are shown in Figure 6 and Figure S2. Compared with the CON group, the height of ileal villi and the ratio of villi to cryptic villi ($P < 0.01$) in the INU group were significantly increased (Figures S2A, B). We found INU and RS groups significantly increased the villi height of the jejunum ($P < 0.05$), but decreased the crypt depth ($P < 0.05$), resulting in a higher ratio of villi to the crypt in the jejunum ($P < 0.01$), compared to the CON group (Figures 3A and 3B).

Furthermore, to explore the protective effect of dietary fiber on intestinal barrier mucosa, we detected the expression level of tight junction protein genes.
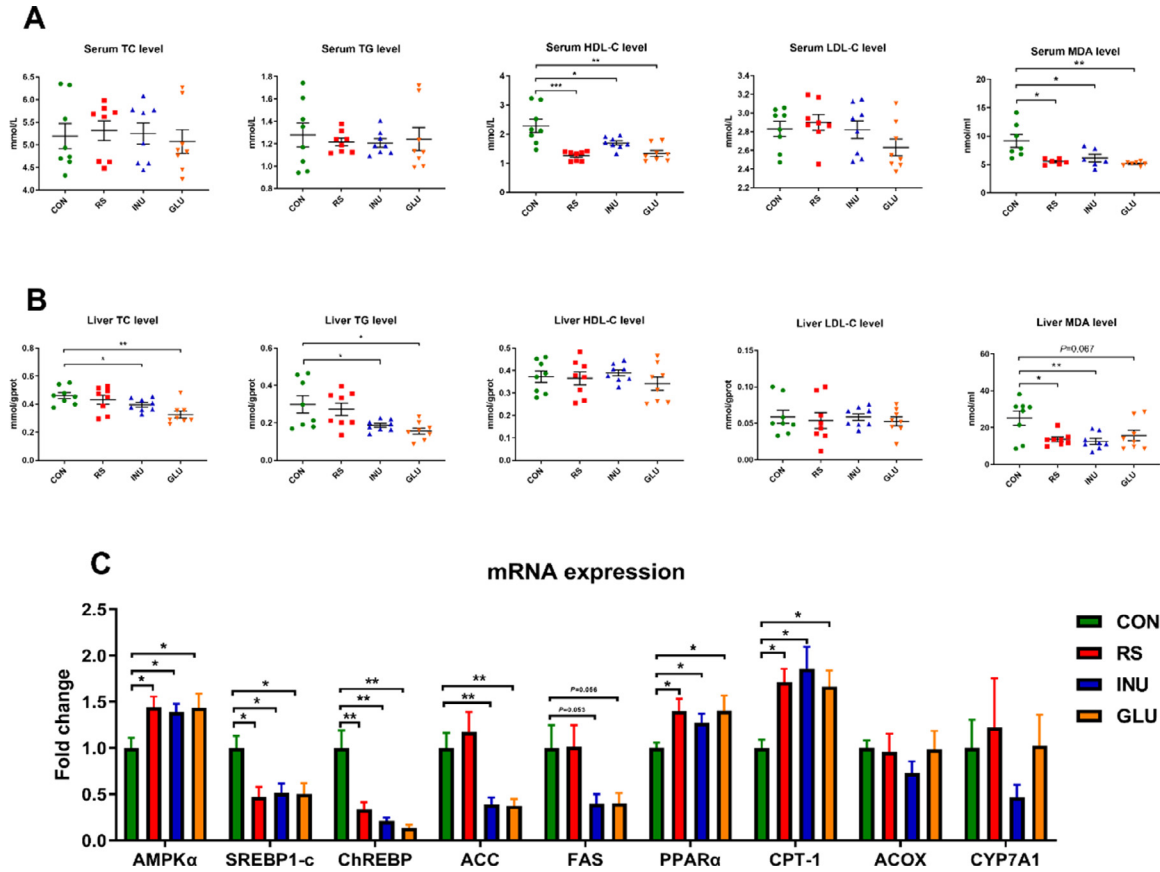
Figure 2. Effects of dietary fiber on lipid metabolism of 15 to 42-day-old Magang geese. (A) Serum biochemical indexes. (B) Liver biochemical indexes. (C) Relative mRNA expressions of lipid metabolism-related genes in the liver of 15 to 42-day-old Magang geese (n = 8, mean with SEM). Data were analyzed with unpaired t test, *$P < 0.05$, **$P < 0.01$, *** $P < 0.001$.

Compared with the CON group, there was no significant difference in the relative expression of the Claudin (**CLDN** 1) gene in all dietary fiber groups. However, the relative expressions of Occludin (**OCLN**), Tight Junction Protein 1 (**TJP**-1), and Rho-associated kinase 1 (**ROCK**-1) in the INU group were significantly increased ($P < 0.05$). The relative expression of the ROCK-1 gene in the RS group was significantly increased ($P = 0.097$, Figure 6C).

DF Supplementation-Induced Drastic Changes in Microbial Diversity and Populations

As shown in Figure 4A, the CON, INU, GLU, and RS groups were well separated, with 13.65 and 7.54% variation explained by principal component PC1 and PC2, respectively. Figure 4B shows that all groups were basically separated from each other at the OTU level by partial least squares discriminant analysis. The alpha diversity was estimated through the ACE index and Chao1 richness estimate. Figures 4C and 4D showed that compared with the CON group, the ACE and Chao1 indexes of INU, GLU, and RS groups were decreased ($P < 0.05$). Results suggested that the composition of cecal microbiota in Magang geese was changed by the DF supplement.

Figures 5A and 5B showed the microbial composition of all groups of geese. Figure 5A shows that *Bacteroides* and *Firmicutes* were predominant phyla in the cecal microbiota, followed by *Proteobacteria, Actinobacteria,* and *Verrucomicrobia*. Relative abundance of gut microbiota composition at the genus level was shown in Figure 5B. Results showed that *Alistipes, Bacteroides, Peptococcus,* and *Parabacteroides* were the predominant genera. At the phyla level, Figures 5C−5F showed that compared with the CON group, the relative abundance of *Bacteroides* in INU ($P < 0.01$) and RS groups ($P < 0.05$) were increased, while the relative abundance of *Proteobacteria* in INU ($P < 0.05$) and RS groups ($P = 0.06$) were decreased. Furthermore, the *Firmicutes / Bacteroides* ratio in INU ($P < 0.05$), GLU ($P = 0.079$), and RS groups ($P < 0.05$) were decreased compared to the CON group.

To further analyze the effect of DFs on the composition of the cecal microflora, we compared the abundance of all groups of microbiota, and identified the main different microflora related to lipid metabolism through cladistogram, linear discriminant analysis effect size (**LEfSe**) analysis: Bacteroides, *Alistipes, Barnesiella, Desulfovibrio, Ruminococcaceae UCG-014,* and *Romboutsia* (Figure 5G and S1). As shown in Figures 5H −5M, at the genus level, RS treatment significantly increased the relative abundances of Bacteroides in geese ($P < 0.01$), while INU and GLU treatment tend to
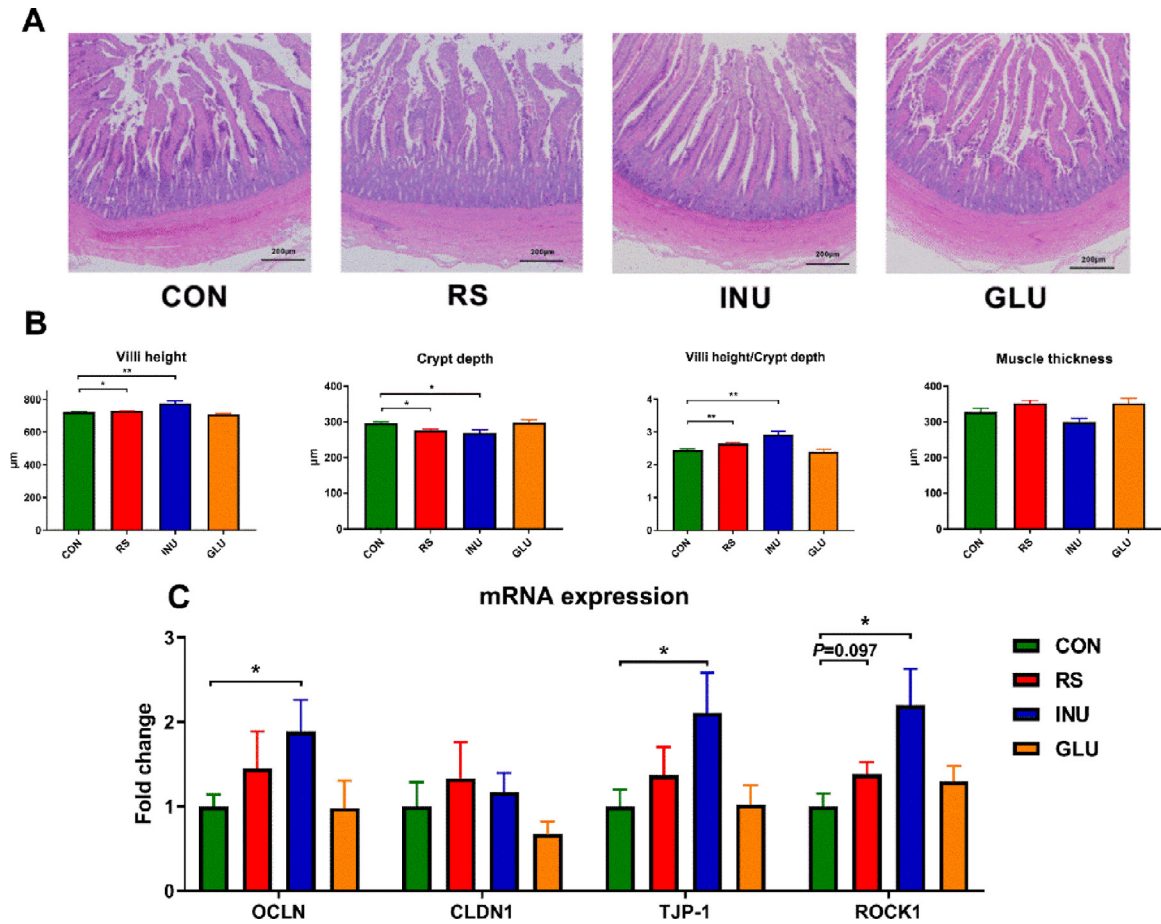
Figure 3. Dietary fiber promotes intestinal morphology and mucosal function. (A) Representative image of H&E staining of jejunum from groups of CON, INU, GLU, and RS (× 40, n = 8). (B) Villi height, crypt depth, the ratio of villi height/crypt depth and muscle thickness of jejunum in different groups (n = 8, mean with SEM). (C) Relative mRNA expressions of *OCLN, CLDN*1, *TJP*-1 and *ROCK*1 in the jejunum of 15 to 42 d Magang geese (n = 8, mean with SEM). Data were analyzed with unpaired t test, *$P < 0.05$, **$P < 0.01$, *** $P < 0.001$.

increase the relative abundances of *Alistipes* ($P = 0.079$ and $P = 0.093$). Compared with the CON group, the relative abundances of *Barnesiella* in INU, GLU, and RS groups were increased ($P < 0.05$ or $P < 0.001$). On the contrary, the relative abundances of *Desulfovibrio* and *Ruminococcaceae UCG-014* in INU, GLU, and RS groups were decreased compared to the CON group ($P < 0.05$ or $P < 0.001$). Meanwhile, the relative abundance of *Romboutsia* was also decreased in the GLU group compared with that in the CON group ($P < 0.05$).

DF Treatment Promotes Generation of SCFAs in Goose

To explore the effects of different DFs on the fermentation products of caecum contents of Magang geese, the main SCFAs, such as acetate, propionate, butyrate, valerate, isobutyrate, and isovalerate were detected. In cecal contents, compared with the CON group, the INU group had significantly higher propionate, butyrate ($P < 0.05$), and higher valerate ($P < 0.01$), the GLU group had higher valerate, isovalerate ($P < 0.05$), and propionate ($P = 0.065$), the RS group had higher acetate, propionate, butyrate, valerate ($P < 0.01$), and isovalerate ($P = 0.065$). Together, the contents of total SCFAs in

the cecum of INU and RS groups were significantly higher than those in the CON group ($P < 0.05$; Figure 6).

Correlation of Gut Microbiota With SCFAs, Lipid Metabolism-Related Indexes

Spearman's correlation analysis was performed to clarify the correlation among the microbiota, SCFAs, and lipid metabolism-related indexes (Figure 7). As shown in Figure 7A, *Barnesiella* and *Ruminococcus_1* were positively correlated with isovalerate, *Romboutsia* were positively correlated with acetate, propionate, and butyrate, whereas *Desulfovibrio* was negatively correlated with propionate and valerate, *Romboutsia* was negatively correlated with isobutyrate and isovalerate, *Ruminococcaceae_ UCG-014* was strongly negatively correlated with isovalerate ($P < 0.01$ or $P < 0.05$), suggesting that they may be the most significant genera for the development of the production of SCFAs. In addition, as shown in Figure 7B, *Bacteroidetes* and *Barnesiella* were positively correlated with *PPARα*, *Desulfovibrio* were strongly positively correlated with *ChREBP* and *FAS, Romboutsia* were positively correlated with liver TC and *ACC*, while *Alistipes* was negatively correlated with liver MDA, *Barnesiella* was highly
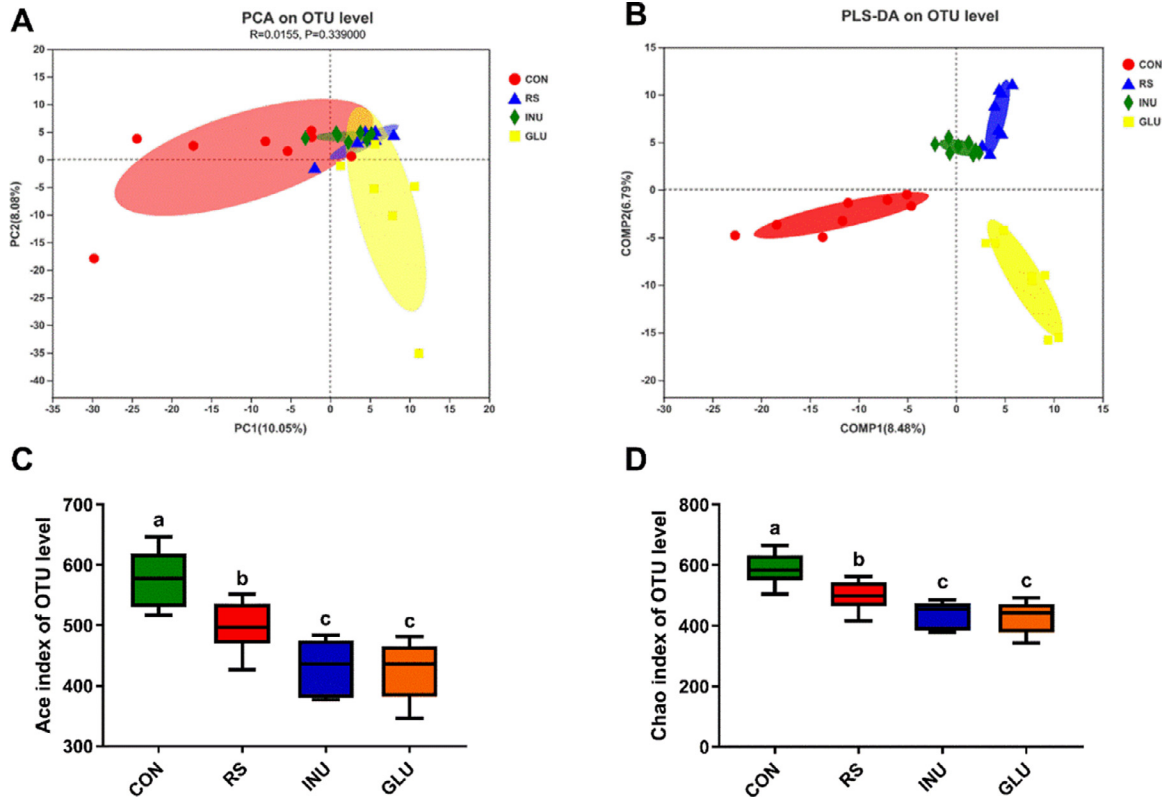
Figure 4. Effect of dietary fiber on cecum microbial diversity of 15 to 42-day-old Magang geese. (A) Principal component analysis (PCA) of microbial communities in the cecum from four groups (n = 8). (B) Partial least squares discriminant analysis of microbial communities in the cecum from four groups (n = 8). (C, D) Alpha diversity: Ace and Chao indexes. Data are expressed as mean ± SEM (n = 8). Error bars represent the standard error of the mean. a, b mean significant difference ($P < 0.05$).

negatively correlated with serum HDL-C, liver TC, liver TG, serum MDA ($P < 0.01$), and ACC ($P < 0.05$), indicating that they may play the most important role in the lipid metabolism.

DISCUSSION

DFs, known as "prebiotics", have gained considerable attention because they withstand digestion in the small intestine and are able to be fermented inside the colon. DFs play key roles in regulating intestinal function and exhibiting beneficial health properties on energy control and body weight (Wnag et al., 2018). In our study, INU, GLU, and RS were respectively added to the diet to evaluate the effects of different viscous DFs on growth performance, intestinal barrier function, lipid metabolism, SCFA production, and bacterial community of Magang geese. It was found that DFs supplementation, especially INU, significantly improves intestinal morphology and enhances the transcription level of intestinal barrier related proteins. In addition, DFs induced remarkable alteration in the diversity of intestinal microbiota and effectively promote the growth of acid-producing bacteria to produce SCFAs, therefore, activated the AMPK pathway by regulating the fatty acid synthesis and β oxidation through the gut-liver axis. Specifically, different types of DFs significantly reduced the content of HDL in serum and improved the peroxidation of Magang geese, manifested in the reduction of MDA.

Growth performance and intestinal structure in livestock and poultry are closely related to DF sources, amount in diets, physical and chemical properties. Previous studies demonstrated that no significant changes were observed on growth performance of piglets in rice husk, cassava meal, bran, fermented bran, and pressed bran diets treatments (Kraier et al., 2015), while diets with sweet potato vine and guar gum decreased porcine daily gain and F/G ratio (Len et al., 2009). Fiber with high viscosity and high lignin content may have a greater resistance impact on the growth performance of animals. However, Yu et al. (2016) reported that diet supplemented with 5% soybean hulls had negative effects on the growth performance of weaned pigs on account of the antinutritional factors, such as trypsin inhibitors and α-galactosides. The porcine experiment showed that a diet with 5% INU improved the villous gland ratio of the front segment of the small intestine. INU also decreased the depth of the hindgut crypt and increased the expression of tight junction protein in piglets. In autoimmune diabetes mellitus and acute pancreatitis models, it was also found that long-chain inulin could improve intestinal barrier function and alleviate disease status by upregulating intestinal connexin and antimicrobial peptides (Molist et al., 2012; Yue et al., 2017). In our study, GLU treatment significantly decreased ADG and ADFI of Magang geese, but increased the relative weight and length of each intestinal segment. Furthermore, compared with the CON group, INU and RS groups significantly increased the
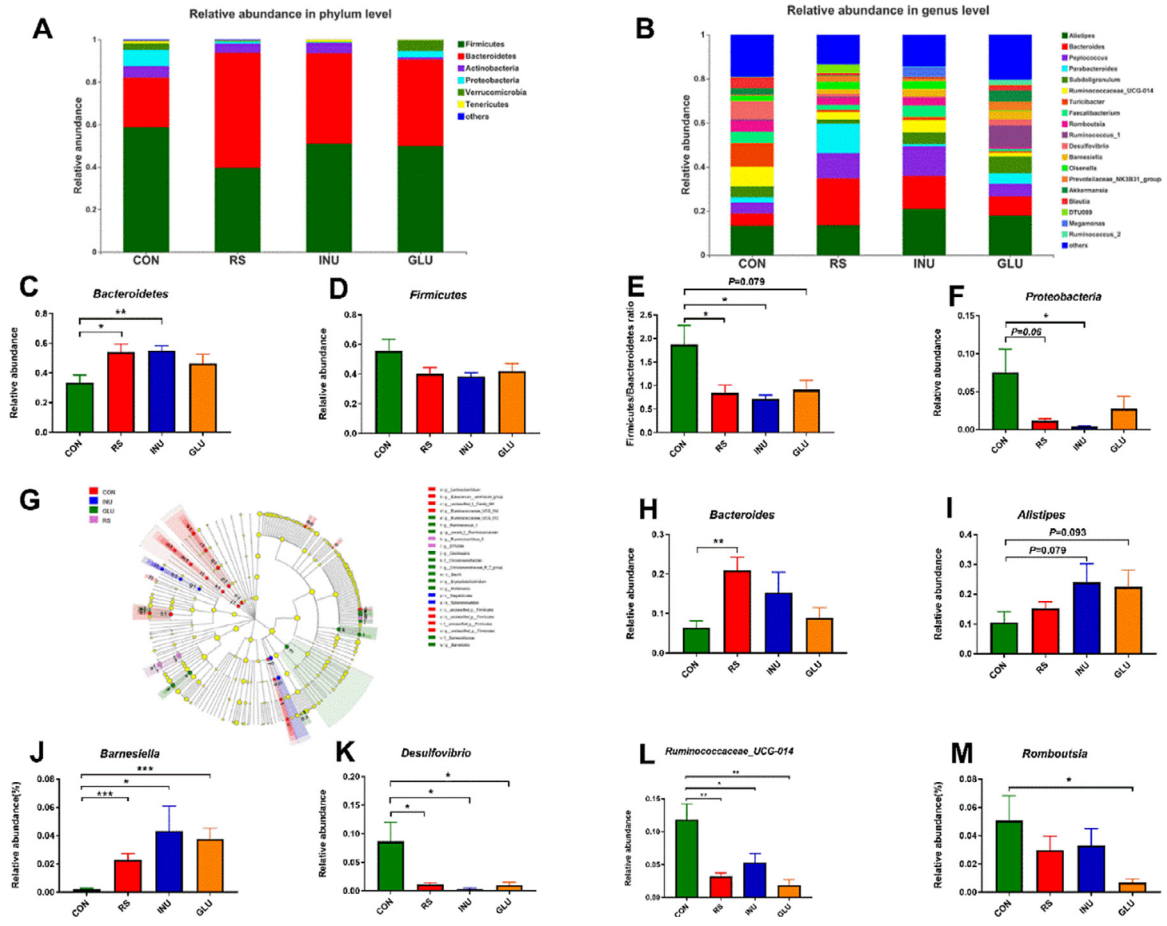
Figure 5. Changes of microbial composition in 15 to 42-day-old Magang geese fed with different types of DF. Microbial composition at the phylum level (A) and genus level (B). Each bar represented the average relative abundance of each bacterial taxon within a group; (C–F) relative abundances of *Bacteroidetes, Firmicutes,* and Proteobacteria in different dietary fiber groups at the phylum level; (G) LEfSe was set up with 0.05 as alpha value for the Wilcoxon test (n = 8); (H–M) relative abundances of *Bacteroides, Alistipes, Barnesiella, Desulfovibrio, Ruminococcaceae_ UCG-014* and *Romboutsia* in different dietary fiber groups at the genus level. Data were analyzed with unpaired *t* test, *$P < 0.05$, **$P < 0.01$, *** $P < 0.001$.

villi height, but decreased the crypt depth, resulting in a higher ratio of villi to the crypt in the jejunum. In addition, it is worth noting that the relative expression of *OCLN, TJP*-1, and *ROCK*-1 genes in the INU group was significantly increased compared to the CON group. This evidence suggested that medium viscosity DF (INU) likely has preferable intestinal mucosal protection to improve intestinal morphology via increasing

intestinal tight junction protein expressions. As we all know, β-glucan has a higher viscosity, which can slow down the gastric emptying rate and intestinal passage rate of feed (Natalia et al., 2013). In addition, it can be fermented by microorganisms to produce SCFAs in the hindgut, and stimulate the secretion of some anorexic hormones, such as casein, glucagon-like peptide-1 (**GLP-1**), which can make the full abdomen feeling,
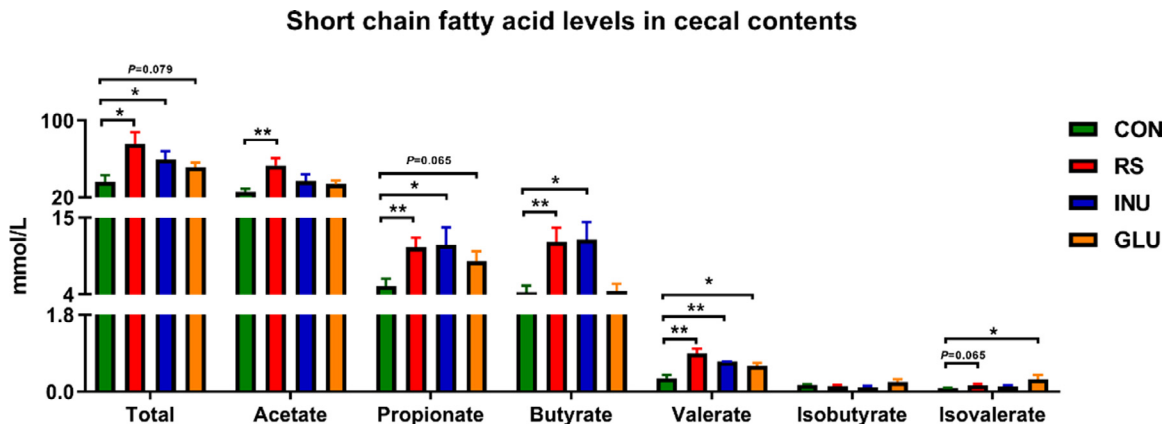

Figure 6. Effect of dietary fiber on short chain fatty acid content of cecal contents in Magang geese aged 15 to 42 d. Data were analyzed with unpaired *t* test, *$P < 0.05$, **$P < 0.01$, *** $P < 0.001$.
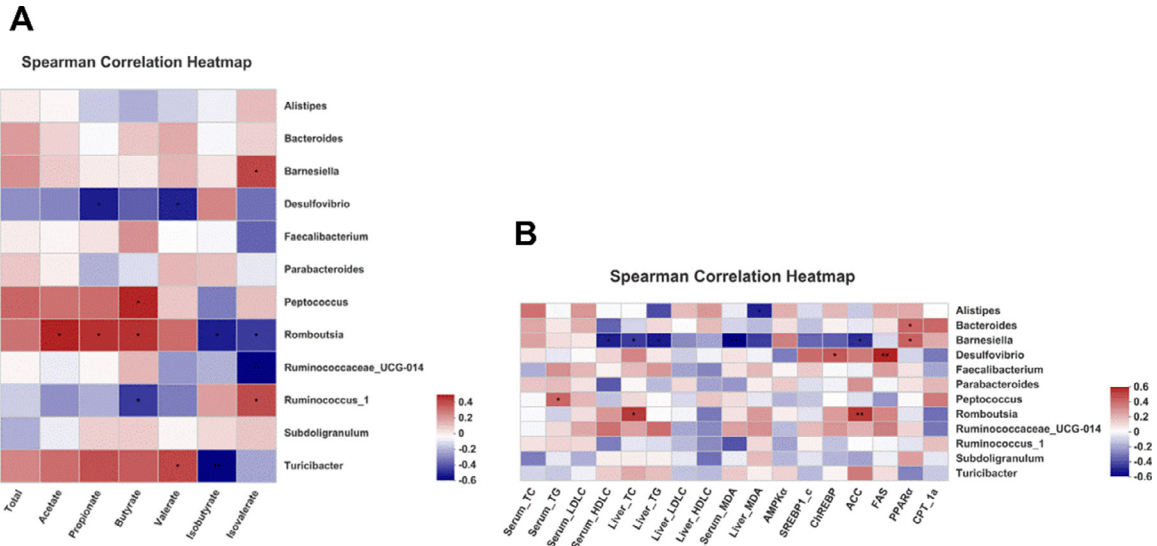
Figure 7. Heatmap of Spearman correlation between cecal microbiota and SCFAs (A). Cecal microbiota and lipid metabolism-related indexes (B). Colors range from blue (negative correlation) to red (positive correlation). Differences were considered statistically significant when $P < 0.05$ (∗, $P < 0.05$; ∗∗, $P < 0.01$; and ∗∗∗, $P < 0.001$; n = 8).

inhibit appetite and reduce the food intake of animals (Adam et al., 2014). An appropriate amount of soluble DFs (INU and GLU) would stimulate intestinal peristalsis, make intestinal villi aligned and increase the height of intestinal villi, therefore resisting the negative effects of high viscosity chyme (Jha et al., 2019). On the other hand, the appropriate amount of insoluble DF with a low degree of lignification can increase villus height and reduce crypt depth of the intestine. SCFAs are fermented by nondigestible carbohydrates through microbiota at the back end of the digestive tract. These compounds especially butyric acid, are likely to contribute to the proliferation of intestinal epithelial cells and improve the morphology of intestinal mucosa (Frampton et al., 2020). Therefore, different fiber sources exerted various effects on the growth performance, the physiological function of the gastrointestinal, and gut health of animals depending upon their physicochemical properties and chemical components.

The liver is the main site of lipid metabolism, which plays an important role in regulating lipid metabolism and lipid homeostasis maintaining (Zhang et al., 2018). As a marker of endogenous lipid peroxidation in the cell, MDA reflects the degree of lipid peroxidation damage in the animal body (Petry et al., 2020). In our study, compared with the CON group, INU, GLU, and RS groups reduced the levels of HDL-C and MDA in serum, as well as the contents of TC, TG, and MDA in the liver, which means that DFs significantly reduced the lipid accumulation in organism. Noticeably, the high viscosity DF (GLU) group has the lowest serum MDA level, as well as liver TC and TG, manifesting a greater lipid-lowering effect on geese. β-glucan from different sources, such as cereal and bacteria, appeared to have positive effects on blood cholesterol-reducing and lipolysis (Zhu et al., 2016; Grundy et al., 2017). Inulin also has the preferable lipid reducing effect compared with resistant starch. In hens, inulin has been proved to reduce abdominal fat

weight, liver weight, and liver cholesterol content (Mohiti et al., 2012). In mice and hamsters, inulin or resistant starch was also found to reduce triglyceride and MDA contents in serum (Hales, 2019).

To further investigate the effect of DFs on lipid metabolism, mRNA levels of genes related to lipogenesis and fatty acid oxidation in the liver were studied. Serves as an energy sensor in lipid metabolism, AMPK has the potential to switch cells from an anabolic to a catabolic state, with inhibiting lipogenesis and increasing fatty acid oxidation in liver (Foretz et al., 2011; Qin et al., 2018). AMPKα, as an energy sensor in lipid metabolism, could inhibit anabolic pathways (SREBP-1c, FAS, and ACC1) and stimulate catabolic pathways (PPARα, CPT-1, and ACOX; Herzig and Shaw, 2018; Yeh et al., 2018). In our results, lipid catabolic processing related genes *AMPKα, PPARα,* and *CPT*-1 mRNA expression was significantly increased in DFs groups ($P < 0.05$). As an activator of *FAS* and *ACC1* in lipogenesis, the dysregulation of *SREBP-1c* has been proved to be involved in dyslipidemia and hepatic steatosis (Herzig and Shaw, 2018). Our results showed that lipid anabolic-related genes, *SREBP-1c, ChREBP, FAS,* and *ACC1,* were almost decreased in INU and GLU treatments in geese. Carnitine palmitoyltransferase (**CPT1A**) and *PPARα* participate in fatty acid β-oxidation, whereas *CPT1A* is a rate-limiting enzyme and *PPARα* could promote the target genes related to fatty acid β-oxidation (Raghow et al., 2008; Kersten and Sander, 2014). As a transcription factor, *ChREBP-1c* has potential importance in the regulation of glucose-dependent lipid production in poultry and regulates the expression of *FAS* and *ACC* (Dong et al., 2017). Some studies have shown that DFs interfere with the signal transduction process of lipogenesis (Proszkowiec-Weglarz et al., 2008; Yin et al., 2011; Si et al., 2017; Shang et al., 2017). RS and ARS (**acetylated resistant starch**) had been demonstrated to reduce the mRNA expressions of

SREBP-1, HMG-CoAR, and ACC in varying degrees (Ribeiro et al., 2019). A study in mice reported the molecular mechanism of RS in improving lipid metabolism and promoting fatty acid β oxidation through the AMPK pathway (Shang et al., 2017). Choi et al (2017) found that the cooked rice (RS3) diet significantly increased PPAR α and downstream mRNA expression of CPT-1 and peroxisomal acyl-coenzyme A oxidase, and therefore, promoted fatty acid β oxidation. Reduced antioxidants and elevated lipid peroxidation have been observed in animal models and NAFLD patients (Serviddio et al., 2013). The regulation of DFs on these genes contributed to a declined lipid biosynthesis and enhanced fatty acid oxidation, thus restraining the lipid accumulation in the liver. DFs decreased the ratio of *SREBP-1c: PPARα*, which has been proposed to prevent the development of hepatic steatosis and NAFLD in obese patients (Pettinelli et al., 2009). Our results suggested that DFs may reduce hepatic lipid accumulation and regulate lipid metabolism-related genes via activation of *AMPKα* and thereby attenuate hepatic steatosis.

The pathogenesis of obesity is closely related to the increased ratio of *Firmicutes/Bacteroidetes* (Paenell and Reimer, 2012; Grigor'eva, 2020). In our study, geese with DFs diet showed a significant decrease in the ratio of *Firmicutes* to *Bacteroidetes*, manifested the correlation of these microbiotas with lower body fat deposition; meanwhile, the relative abundances of *Bacteroidetes* in INU and RS groups were significantly higher than that in the CON group. A similar study found that inulin and oligofructose supplementation could mitigate gut microbiota imbalance including lowering the ratio of *Firmicutes-to-Bacteroidetes.* As a major phylum of Gram-negative bacteria in the intestine, Proteobacteria consists of a large number of pathogens with an outer membrane composed of lipopolysaccharides (**LPS**). Obesity is also characterized as endotoxemia because of the release of LPS into circulation (Klein et al., 2007). Accordingly, Proteobacteria phylum are usually enriched in obesity and metabolic diseases (Zhang et al., 2012). Our current results showed that the relative abundance of Proteobacteria significantly decreased in the INU and RS group ($P < 0.05$ or $P = 0.06$). In HFD mice, *Bacteroides* and *Barnesiella* are negatively correlated with obesity (Kan et al., 2020). The abundance of *Alistipes* has a significant negative correlation with body weight, TC, TG, HDL-C, LDL-C, and blood glucose of mice (Liu et al., 2016). Specifically, the LPS-producing microbiota such as *Desulfovibrio* became abundant in mice models after HFD feeding (Li et al., 2018). *Desulfovibrio* is one kind of genus belonging to *Desulfovibrionaceae* and Proteobacteria, positively related to obesity-induced inflammation (Lennon et al., 2014). In addition, an increased abundance of *Ruminococcaceae* characterizes dysbiosis in patients with inflammatory bowel syndrome (Rajili et al., 2015). 1-Deoxynojirimycin treatment relieved gut dysbiosis in diabetic mice by suppressing the growth of *Ruminococcaceae UCG-014* (Hu et al.,

2019). *Romboutsia*, positively correlated with fat metabolism and enriched in the HFD group, could effectively promote fat decomposition and absorption (Martinez-Guryn et al., 2018). Our data showed that DFs treatment changes intestinal microbial composition in geese by promoting the growth of Bacteroidetes, *Bacteroides, Alistipes,* and *Barnesiella* and suppressing the growth of Proteobacteria, *Desulfovibrio, Ruminococcaceae_ UCG-014,* and *Romboutsia.* These results indicated that DFs could upregulate the abundance of beneficial gut microbial communities associated with antiobesity, thus playing a critical role in activating lipid metabolism.

SCFAs are the major gut microbial metabolites of nondigestible carbohydrate fermentation by the gut microbiota (Weitkunat et al., 2015). Several studies have demonstrated the ability of SCFAs to induce the phosphorylation of AMPK in myotubes and skeletal muscle (Gao et al., 2009; Pan et al., 2015; Hong et al., 2016), probably because of the increase of AMP concentrations and the AMP/ATP ratio within skeletal muscle tissue mediated by SCFA (Yamashita et al., 2009; Hong et al., 2016). As shown in our study, the concentrations of total SCFAs were significantly increased in three DFs groups. In cecal contents, compared with the CON group, the INU group had significantly higher propionate, butyrate ($P < 0.05$), and higher valerate ($P < 0.01$), the GLU group had higher valerate, isovalerate ($P < 0.05$), and propionate ($P = 0.065$), the RS group had higher acetate, propionate, butyrate, valerate ($P < 0.01$) and isovalerate ($P = 0.065$). Importantly, AMPK activation can produce a metabolic milieu similar to that generated by SCFA administration. This milieu is characterized by an increase in fatty acid uptake and oxidation, glucose uptake and glycogenesis, and inhibition of lipogenesis and glycolysis (Mihaylova and Shaw, 2011). Increasing evidence suggested that SCFAs have beneficial effects on body weight control and lipid homeostasis (Chambers et al., 2018; Zhao et al., 2019). Butyric acid produced by dietary fiber fermentation in the gut is mainly metabolized in intestinal cells (Kohji and Tomio), while acetic acid and propionic acid are transported to the liver through portal vein blood (Dalile et al., 2019). High-dietary fiber intake significantly improved the SCFA levels, including acetate, propionate, butyrate, and isovalerate in HFD-fed mice after lactation (Liu et al., 2020). Studies in humans and animals have found that propionic acid also is used as the main substrate for de novo synthesis of fat (Bloemen et al., 2009; Sun et al., 2016). These results showed that DFs may increase the production of SCFAs by increasing the populations of SCFA-producing bacteria. For example, *Bacteroidetes* ferments lactic acid and glucose into propionate and acetate, and *Barnesiella* was one of the main butyrate-producing microorganisms (Moreno-Indias et al., 2016).

The rapid growth of poultry reduces the amount of intramuscular fat deposition and increases the deposition of subcutaneous fat and abdominal fat, resulting in the decline of meat quality. High abdominal fat not only

affects poultry processing, but also reduces poultry carcass quality, slaughter rate and economic benefits (Khan et al., 2015). Intramuscular fat content is positively correlated with muscle shear force, flavor, and tenderness, which is an important index to measure meat quality (Frank et al., 2016). Lipid, as an important flavor precursor, mainly causes the difference in poultry flavor through lipid oxidation and the interaction between lipid oxidation and Maillard reaction in thermal reaction (Hellwig et al., 2014). Therefore, in practical application, relevant functional substances or plants rich in this component can be added to the diet to regulate the lipid metabolism of poultry. It will be of great significance to further explore the differences of related genes in regulating lipid metabolism in different parts of poultry, the effects of some functional substances on signal transduction pathway and the transformation mechanism of flavor substances in thermal reaction.

In conclusion, our results suggested that lipid metabolism may be associated with SCFAs and alteration of intestinal microbiota induced by DFs with different viscosity. DFs regulate the diversity of the intestinal microbial community and the content of SCFAs, activate the AMPK pathway through the gut-liver axis, then regulate lipid metabolism and body lipid indicators. Therefore, the present study indicates high viscous DF has a greater lipid-lowering effect on geese, and medium viscous DF has preferable intestinal mucosal protection. DFs with different viscosity can be used in the development of functional foods for preventing steatosis and NAFLD.

DISCLOSURES

The authors declare that they have no known competing financial interests or personal relationships that could have appeared to influence the work reported in this paper.

SUPPLEMENTARY MATERIALS

Supplementary material associated with this article can be found, in the online version, at doi:10.1016/j.psj.2022.101742.

REFERENCES

Adam, C. L., P. A. Williams, M. J. Dalby, K. Garden, L. M. Thomson, A. J. Richardson, S. W. Gratz, and A. W Ross. 2014. Different types of soluble fermentable dietary fibre decrease food intake, body weight gain and adiposity in young adult male rats. Nutr. Metab. 11:36.

Bäckhed, F., and J. L. Sonnenburg. 2016. Diet-microbiota interactions as moderators of human metabolism. Nature 535:56–64.

Bloemen, J. G., K. Venema, M. C. van de Poll, S. W. Olde Damink, W. A. Buurman, and C. H Dejong. 2009. Short chain fatty acids exchange across the gut and liver in humans measured at surgery. Clin. Nutr. 28:657–661.

Chambers, E. S., C. S. Byrne, K. Aspey, Y. Chen, S. Khan, D. J. Morrison, and G. Frost. 2018. Acute oral sodium propionate supplementation raises resting energy expenditure and lipid oxidation in fasted humans. Diabetes Obes. Metab. 20:1034–1039.

Choi, J. H., S. W. Kim, R. Yu, and J. W Yun. 2017. Monoterpene phenolic compound thymol promotes browning of 3T3-L1 adipocytes. Eur. J. Nutr. 56:2329–2341.

Dalile, B., L. Van Oudenhove, B. Vervliet, and K. Verbeke. 2019. The role of short-chain fatty acids in microbiota-gut-brain communication. Nat. Rev. Gastroenterol. Hepatol. 16:461–478.

Delitala, A. P., G. Fanciulli, M. Maioli, and G. Delitala. 2017. Subclinical hypothyroidism, lipid metabolism and cardiovascular disease. Eur. J. Intern. Med. 38:17–24.

Dong, Z., P. Zhao, M. Xu, C. Zhang, W. Guo, H. Chen, J. Tian, H. Wei, R. Lu, and T. Cao. 2017. Astragaloside IV alleviates heart failure via activating PPARα to switch glycolysis to fatty acid β-oxidation. Sci. Rep 7:2691.

Engeli, S., R. Stinkens, T. Heise, M. May, G. H. Goossens, E. E. Blaak, B. Havekes, T. Jax, D. Albrecht, P. Pal, U. Tegtbur, S. Haufe, T. H. Langenickel, and J. Jordan. 2018. Effect of sacubitril/valsartan on exercise-induced lipid metabolism in patients with obesity and hypertension. Hypertension 71:70–77.

Foretz, M., and B. Viollet. 2011. Regulation of hepatic metabolism by AMPK. J. Hepatol. 54:827–829.

Frampton, J., K. G. Murphy, G. Frost, and E. S Chambers. 2020. Short-chain fatty acids as potential regulators of skeletal muscle metabolism and function. Nat. Metab. 2:840–848.

Frank, D., S. T. Joo, and R. Warner. 2016. Consumer acceptability of intramuscular fat. Korean J. Food Sci. An 36:699–708.

Gao, Z., J. Yin, J. Zhang, R. E. Ward, R. J. Martin, M. Lefevre, W. T. Cefalu, and J. Ye. 2009. Butyrate improves insulin sensitivity and increases energy expenditure in mice. Diabetes 58:1509–1517.

Grigor'eva, I. N. 2020. Gallstone disease, obesity and the firmicutes/bacteroidetes ratio as a possible biomarker of gut dysbiosis. J. Pers. Med. 11:13.

Grundy, M., J. Quint, A. Rieder, S. Ballance, C. A. Dreiss, K. L. Cross, R. Gray, B. H. Bajka, P. J. Butterworth, P. R. Ellis, and P. J Wilde. 2017. The impact of oat structure and β-glucan on in vitro lipid digestion. J. Funct. Food. 38(Pt A):378–388.

Hales, K. E. 2019. Relationships between digestible energy and metabolizable energy in current feedlot diets. Transl. Anim. Sci 3:945–952.

Hellwig, M., and T. Henle. 2014. Baking, ageing, diabetes: a short history of the Maillard reaction. Angew. Chem. Int. Edit 53:10316–10329.

Herzig, S., and R. J Shaw. 2018. AMPK: guardian of metabolism and mitochondrial homeostasis. Nat. Rev. Mol. Cell Biol. 19:121–135.

Hong, J., Y. Jia, S. Pan, L. Jia, H. Li, Z. Han, D. Cai, and R. Zhao. 2016. Butyrate alleviates high fat diet-induced obesity through activation of adiponectin-mediated pathway and stimulation of mitochondrial function in the skeletal muscle of mice. Oncotarget 7:56071–56082.

Hooda, S., B. U. Metzler-Zebeli, T. Vasanthan, and R. T Zijlstra. 2011. Effects of viscosity and fermentability of dietary fibre on nutrient digestibility and digesta characteristics in ileal-cannulated grower pigs. Br. J. Nutr. 106:664–674.

Hu, T. G., P. Wen, W. Z. Shen, F. Liu, Q. Li, E. N. Li, S. T. Liao, H. Wu, and Y. X Zou. 2019. Effect of 1-deoxynojirimycin isolated from mulberry leaves on glucose metabolism and gut microbiota in a streptozotocin-induced diabetic mouse model. J. Nat. Prod. 82:2189–2200.

Jha, R., J. M. Fouhse, U. P. Tiwari, L. Li, and B. P Willing. 2019. Dietary fiber and intestinal health of monogastric animals. Front. Vet. Sci. 6:48.

Kan, J., C. Chen, T. Huo, W. Xie, and C. H Jin. 2020. Polyphenolic-enriched peach peels extract regulates lipid metabolism and improves the gut microbiota composition in high fat diet-fed mice. J. Funct. Food. 72:104082.

Kersten, S. 2014. Integrated physiology and systems biology of PPARα. Mol. Metab. 3:354–371.

Khan, M. I., C. Jo, and M. R. Tariq. 2015. Meat flavor precursors and factors influencing flavor precursors—a systematic review. Meat Sci. 110:278–284.

Klein, S., D. B. Allison, S. B. Heymsfield, D. E. Kelley, R. L. Leibel, C. Nonas, and R. Kahn. 2007. Association for Weight Management and Obesity Prevention, NAASO, Obesity Society, American Society for Nutrition, and American Diabetes Association. 2007. Waist circumference and cardiometabolic risk: a consensus statement from shaping America's health: Association for Weight Management and Obesity Prevention; NAASO, the Obesity Society; the American Society for Nutrition; and the American Diabetes Association. Diabetes Care 30:1647–1652.

Kraler, M., K. Schedle, C. Schwarz, K. J. Domig, M. Pichler, A. Oppeneder, W. Wetscherek, M. Prückler, M. Pignitter, K. F. Pirker, V. Somoza, D. Heine, and W. Kneifel. 2015. Fermented and extruded wheat bran in piglet diets: impact on performance, intestinal morphology, microbial metabolites in chyme and blood lipid radicals. Arch. Anim. Nutr. 69:378–398.

Len, N. T., T. T. Hong, B. Ogle, and J. E Lindberg. 2009. Comparison of total tract digestibility, development of visceral organs and digestive tract of Mong cai and Yorkshire x Landrace piglets fed diets with different fibre sources. J. Anim. Physiol. Anim. Nutr. 93:181–191.

Lennon, G., Á. Balfe, N. Bambury, A. Lavelle, A. Maguire, N. G. Docherty, J. C. Coffey, D. C. Winter, K. Sheahan, and P. R O'Connell. 2014. Correlations between colonic crypt mucin chemotype, inflammatory grade and Desulfovibrio species in ulcerative colitis. Colorectal Dis 16:161–169.

Li, S., J. Li, G. Mao, T. Wu, Y. Hu, X. Ye, D. Tian, R. J. Linhardt, and S. Chen. 2018. A fucoidan from sea cucumber Pearsonothuria graeffei with well-repeated structure alleviates gut microbiota dysbiosis and metabolic syndromes in HFD-fed mice. Food Funct 9:5371–5380.

Liu, Z., Z. Chen, H. Guo, D. He, H. Zhao, Z. Wang, W. Zhang, L. Liao, C. Zhang, and L. Ni. 2016. The modulatory effect of infusions of green tea, oolong tea, and black tea on gut microbiota in high-fat-induced obese mice. Food Funct 7:4869–4879.

Liu, Z., L. Li, S. Ma, J. Ye, H. Zhang, Y. Li, A. T. Sair, J. Pan, X. Liu, X. Li, S. Yan, and X. Liu. 2020. High-dietary fiber intake alleviates antenatal obesity-induced postpartum depression: roles of gut microbiota and microbial metabolite short-chain fatty acid involved. J. Agric. Food Chem. 68:13697–13710.

Martinez-Guryn, K., N. Hubert, K. Frazier, S. Urlass, M. W. Musch, P. Ojeda, J. F. Pierre, J. Miyoshi, T. J. Sontag, C. M. Cham, C. A. Reardon, V. Leone, and E. B Chang. 2018. Small intestine microbiota regulate host digestive and absorptive adaptive responses to dietary lipids. Cell Host Microbe 23:458–469.

Mihaylova, M. M., and R. J. Shaw. 2011. The AMPK signalling pathway coordinates cell growth, autophagy and metabolism. Nat. Cell Biol. 13:1016–1023.

Mohiti-Asli, M., M. Shivazad, M. Zaghari, S. Aminzadeh, M. Rezaian, and G. G Mateos. 2012. Dietary fibers and crude protein content alleviate hepatic fat deposition and obesity in broiler breeder hens. Poult. Sci. 91:3107–3114.

Molist, F., E. G. Manzanilla, J. F. Pérez, and C. M Nyachoti. 2012. Coarse, but not finely ground, dietary fibre increases intestinal Firmicutes:Bacteroidetes ratio and reduces diarrhoea induced by experimental infection in piglets. Br. J. Nutr. 108:9–15.

Moreno-Indias, I., L. Sánchez-Alcoholado, P. Pérez-Martínez, C. Andrés-Lacueva, F. Cardona, F. Tinahones, and M. I. Queipo-Ortuño. 2016. Red wine polyphenols modulate fecal microbiota and reduce markers of the metabolic syndrome in obese patients. Food Funct 7:1775–1787.

Müller, M., E. E. Canfora, and E. E. Blaak. 2018. Gastrointestinal transit time, glucose homeostasis and metabolic health: modulation by dietary fibers. Nutrients 10:275.

Natalia, S., M. Len, and G. Daniel. 2013. The role of viscosity and fermentability of dietary fibers on satiety- and adiposity-related hormones in rats. Nutrients 5:2093–2113.

Pan, J. H., J. H. Kim, H. M. Kim, E. S. Lee, D. H. Shin, S. Kim, M. Shin, S. H. Kim, J. H. Lee, and Y. J Kim. 2015. Acetic acid enhances endurance capacity of exercise-trained mice by increasing skeletal muscle oxidative properties. Biosci. Biotechnol. Biochem. 79:1535–1541.

Parnell, J. A., and R. A Reimer. 2012. Prebiotic fibres dose-dependently increase satiety hormones and alter Bacteroidetes and Firmicutes in lean and obese JCR:LA-cp rats. Br. J. Nutr. 107:601–613.

Paturi, G., C. Butts, J. Monro, K. Nones, S. Martell, R. Butler, and J. Sutherland. 2010. Cecal and colonic responses in rats fed 5 or 30% corn oil diets containing either 7.5% broccoli dietary fiber or microcrystalline cellulose. J. Agric. Food Chem. 58:6510–6515.

Petry, A. L., N. F. Huntley, M. R. Bedford, and J. F Patience. 2020. Xylanase increased the energetic contribution of fiber and improved the oxidative status, gut barrier integrity, and growth performance of growing pigs fed insoluble corn-based fiber. J. Anim. Sci. 98:skaa233.

Pettinelli, P., T. Del Pozo, J. Araya, R. Rodrigo, A. V. Araya, G. Smok, A. Csendes, L. Gutierrez, J. Rojas, O. Korn, F. Maluenda, J. C. Diaz, G. Rencoret, I. Braghetto, J. Castillo, J. Poniachik, and L. A Videla. 2009. Enhancement in liver SREBP-1c/PPAR-alpha ratio and steatosis in obese patients: correlations with insulin resistance and n-3 long-chain polyunsaturated fatty acid depletion. Biochim. Biophys. Acta 1792:1080–1086.

Proszkowiec-Weglarz, M., B. D. Humphrey, and M. P Richards. 2008. Molecular cloning and expression of chicken carbohydrate response element binding protein and Max-like protein X gene homologues. Mol. Cell. Biochem. 312:167–184.

Qin, W., B. Zhou, G. Yang, W. Hu, L. Zhang, L. Rui, M. Li, K. Wang, H. F. Gu, and Y. Guan. 2018. JAZF1 ameliorates age and diet-associated hepatic steatosis through SREBP-1c -dependent mechanism. Cell Death Dis. 9:859.

Raghow, R., C. Yellaturu, X. Deng, E. A. Park, and M. B Elam. 2008. SREBPs: the crossroads of physiological and pathological lipid homeostasis. Trends Endocrinol. Metab. 19:65–73.

Rajilić-Stojanović, M., D. M. Jonkers, A. Salonen, K. Hanevik, J. Raes, J. Jalanka, W. M. de Vos, C. Manichanh, N. Golic, P. Enck, E. Philippou, F. A. Iraqi, G. Clarke, R. C. Spiller, and J. Penders. 2015. Intestinal microbiota and diet in IBS: causes, consequences, or epiphenomena? Am. J. Gastroenterol. 110:278–287.

Ribeiro, É. M., M. C. Peixoto, T. C. Putarov, M. Monti, P. Pacheco, B. A. Loureiro, G. T. Pereira, and A. C Carciofi. 2019. The effects of age and dietary resistant starch on digestibility, fermentation end products in faeces and postprandial glucose and insulin responses of dogs. Arch. Anim. Nutr. 73:485–504.

Serviddio, G., F. Bellanti, and G. Vendemiale. 2013. Free radical biology for medicine: learning from nonalcoholic fatty liver disease. Free Radic. Biol. Med. 65:952–968.

Shang, W., X. Si, P. Strappe, Z. Zhou, and C. Blanchard. 2017. Resistant starch attenuates impaired lipid biosynthesis induced by dietary oxidized oil via activation of insulin signaling pathways. RSC Adv 7:50772–50780.

Si, X., Z. Zhou, P. Strappe, and C. Blanchard. 2017. A comparison of RS4-type resistant starch to RS2-type resistant starch in suppressing oxidative stress in high-fat-diet-induced obese rats. Food Funct 8:232–240.

Sun, Y., K. Yu, L. Zhou, L. Fang, Y. Su, and W. Zhu. 2016. Metabolomic and transcriptomic responses induced in the livers of pigs by the long-term intake of resistant starch. J. Anim. Sci. 94:1083–1094.

Wang, G., Q. Xu, X. Jin, H. Fe Ng, Z. Liu, and J. Zhao. 2018. Effects of lactobacilli with different regulatory behaviours on tight junctions in mice with dextran sodium sulphate-induced colitis. J. Funct. Food. 47:107–115.

Wang, J., and H. Jia. 2016. Metagenome-wide association studies: fine-mining the microbiome. Nat. Rev. Microbiol. 14:508–522.

Weitkunat, K., S. Schumann, K. J. Petzke, M. Blaut, G. Loh, and S. Klaus. 2015. Effects of dietary inulin on bacterial growth, short-chain fatty acid production and hepatic lipid metabolism in gnotobiotic mice. J. Nutr. Biochem. 26:929–937.

Wu, W., J. Hu, H. Gao, H. Chen, X. Fang, H. Mu, Y. Han, and R. Liu. 2020. The potential cholesterol-lowering and prebiotic effects of bamboo shoot dietary fibers and their structural characteristics. Food Chem 332:127372.

Yamashita, H., H. Maruta, M. Jozuka, R. Kimura, H. Iwabuchi, M. Yamato, T. Saito, K. Fujisawa, Y. Takahashi, M. Kimoto, M. Hiemori, and H. Tsuji. 2009. Effects of acetate on lipid metabolism in muscles and adipose tissues of type 2 diabetic Otsuka Long-Evans Tokushima Fatty (OLETF) rats. Biosci. Biotechnol. Biochem. 73:570–576.

Yeh, Y. T., Y. Y. Cho, S. C. Hsieh, and A. N Chiang. 2018. Chinese olive extract ameliorates hepatic lipid accumulation in vitro and in vivo by regulating lipid metabolism. Sci. Rep 8:1057.

Yin, F., Y. Yin, Z. Zhang, M. Xie, J. Huang, R. Huang, and T. Li. 2011. Digestion rate of dietary starch affects the systemic circulation of lipid profiles and lipid metabolism-related gene expression in weaned pigs. Br. J. Nutr. 106:369–377.

Yu, C., S. Zhang, Q. Yang, Q. Peng, J. Zhu, X. Zeng, and S. Qiao. 2016. Effect of high fibre diets formulated with different fibrous ingredients on performance, nutrient digestibility and faecal microbiota of weaned piglets. Arch. Anim. Nutr. 70:263–277.

Yue, H., C. Wu, J. Li, H. Li, Z. Sun, Z. Hao, D. V. Paul, L. L. Pan, and S. Jia. 2017. Inulin-type fructans modulates pancreatic−gut innate immune responses and gut barrier integrity during experimental acute pancreatitis in a chain length-dependent manner. Front Immunol 8:1209.

Zhang, C., J. Seo, K. Murakami, E. Salem, E. Bernhard, V. J. Borra, K. Choi, C. L. Yuan, C. C. Chan, X. Chen, T. Huang, M. T. Weirauch, S. Divanovic, N. R. Qi, H. E. Thomas, C. A. Mercer, H. Siomi, and T. Nakamura. 2018. Hepatic Ago2-mediated RNA silencing controls energy metabolism linked to AMPK activation and obesity-associated pathophysiology. Nat. Commun. 9:3658.

Zhang, X., Y. Zhao, M. Zhang, X. Pang, J. Xu, C. Kang, M. Li, C. Zhang, Z. Zhang, Y. Zhang, X. Li, G. Ning, and L. Zhao. 2012. Structural changes of gut microbiota during berberine-mediated prevention of obesity and insulin resistance in high-fat diet-fed rats. PLoS One 7:e42529.

Zhao, Y., M. A. Evans, A. G. Bertoni, M. J. Budoff, M. H. Criqui, P. Ouyang, J. F. Polak, and N. D Wong. 2019. Multisite atherosclerosis in subjects with metabolic syndrome and diabetes and relation to cardiovascular events: the multi-ethnic study of atherosclerosis. Atherosclerosis 282:202–209.

Zhou, H., W. Guo, T. Zhang, B. Xu, D. Zhang, Z. Teng, D. Tao, Y. Lou, and Y. Gao. 2018. Response of goose intestinal microflora to the source and level of dietary fiber. Poult. Sci. 97:2086–2094.

Zhu, Y., Y. Yao, Y. Gao, Y. Hu, Z. Shi, and G. Ren. 2016. Suppressive effects of barley β-glucans with different molecular weight on 3T3-L1 adipocyte differentiation. J. Food Sci. 81:H786–H793.